



UDC 655:535.361; 535.555

DOI: 10.20535/2077-7264.4(78).2022.274216

© **M. Horskyi, PhD in physics and mathematics science, Associate professor, K. Zenkova, Doctor of physics and mathematics of science, Professor, V. Morfliuk-Shchur, PhD in technical science, Assistant, O. Dubolazov, Doctor of physics and mathematics of science, Professor, L. Slotska, PhD in technical science, Associate professor, A. Dovhun, PhD in physics and mathematics science, Associate professor, Yu. Tomka, PhD in physics and mathematics science, Associate professor, Chernivtsi National University, Chernivtsi, Ukraine**

APPLIED SOFTWARE SPACE-FREQUENCY PROCESSING OF GRAPHIC INFORMATION FOR STANDARDIZATION OF PRINTING MATERIALS OF PACKAGING PRODUCTS

We have proposed a new polarimetric method of Stokes polarimetry, which is more informative in terms of representing optically inhomogeneous structures by spatially coherent filtering.

Keywords: applied programming; graphic information processing; metrology and standardization; publishing and printing; packaging materials; materials science.

Introduction

By using laser coherent radiation, the methods of correlometry and interferometry for measuring the distributions of amplitudes and phases in scattered polarization fields have been widely developed [1, 2]. The main parameters of such coherent fields is the state of polarization resulting from the superposition of orthogonally polarized and phase-shifted amplitudes of partial laser waves [3].

The main result of this approach is the development of a new technique for optical diagnostics, laser polarimetry of polarization-inhomogeneous layers [4–8].

The technique of this type of diagnostics is based on the assump-

tion that the structure of a polymer consists of two main components, an isotropic and a linear birefringent network, which is formed by spatially ordered molecular formations of polymers.

For further universalization of such a model, it is proposed to use the Stokes polarimetric method, which is more informative in terms of displaying inhomogeneous structures using spatial-frequency filtering.

This approach is based on the use of spatial frequency filtering of optically inhomogeneous polarization images of polymer layers.

In our work, we present the results of an experimental verification of a new method of Fourier correlation polarimetry of the frequency



spectra of optical images, which is based on a statistical analysis of inhomogeneous maps with the determination of a set of statistical moments of 1–4 orders that characterize the distribution data.

Method

On fig. 1 are presented a schematic representation of the experimental setup of the Stokes polarimeter using the direct Fourier transform FFT [9, 10].

Irradiation was carried out by a parallel ($\varnothing = 10^4 \mu\text{m}$) beam of a He-Ne laser ($\lambda = 0,6328 \mu\text{m}$; $W = 5\text{mW}$ power).

The polarizing source consists of quarter-wave plates 3, 5 and a polarizer (analyzer) 4, which ensures the formation of a laser beam with an arbitrary polarization azimuth $0^\circ \leq \alpha_0 \leq 180^\circ$ or ellipticity $0^\circ \leq \beta_0 \leq 90^\circ$.

The polymer samples were located in the focal plane of the objective 7 (focal length of objective $f = 30 \text{ mm}$, magnification — 4X, digital aperture N. A. = 0,1), projected into the plane of the light-sensitive plane, $N = m \times n = 800 \times 600$ pixel size, CCD-camera 10, which was also at the focal length of the

objective and provided a range of the Fourier spectrum elements of the polymer images for geometric dimensions $2 \mu\text{m} - 2000 \mu\text{m}$.

The experimental tasks were chosen in such a way as to practically eliminate spatial-angular aperture filtering in the formation of Fourier (FFT) spectra of laser polymer layers images. That was ensured by matching the angular characteristics of the scattering light indicatrices by the polymer samples ($\Omega_{\text{БТ}} \approx 16^\circ$) and the angular aperture of the microobjective ($\Delta\omega = 20^\circ$). Here $\Omega_{\text{БТ}}$ — the angular weak of indicatrices, in which 98 % of the total energy of the scattered radiation is concentrated.

The analysis of the Fourier spectra polarization structure of the images of the polymer layers samples was carried out using a polarizer (9) and a quarter-wave plate (8).

The possibility of determining XY distributions of the Stokes vector parameters in the Fourier plane of two types samples of polyethylene is considered:

— group 1 — with mechanical deformation (stretching), fig. 2, a;

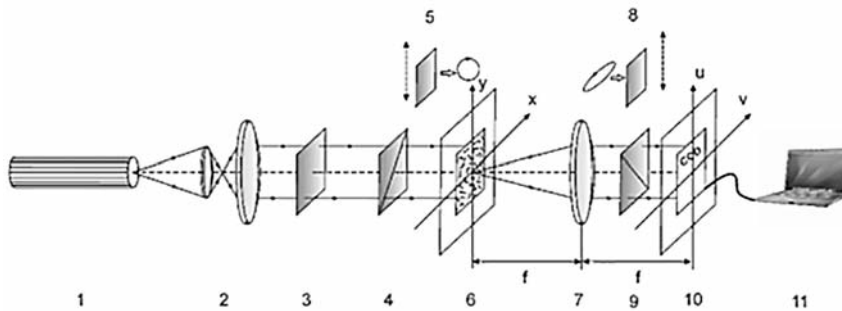


Fig. 1. Optical scheme of Stokes polarimetr, where 1 — He-Ne laser; 2 — collimator; 3 — quarter-wave stationary plate; 4, 9 — polarizer and analyzer, respectively; 5, 8 — quarter-wave plates; 6 — objects plane; 7 — microlens; 10 — CCD; 11 — Personal Computer

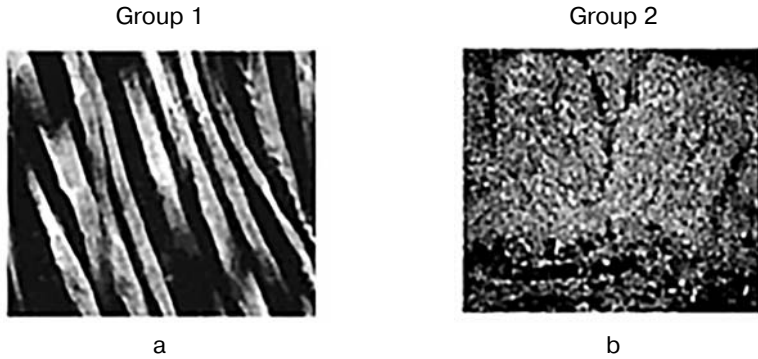


Fig. 2. Image of polarization visualized (in 0–90° polarizer and analyzer) birefringent structure of polyethylene samples from both groups

— group 2 — heat-treated, fig. 2, b.

In general, for each jk -pixel of a CCD camera, one can determine the Stokes vector magnitude of polarization field by making six intensity measurements under these polarization filtering conditions:

— First one — orient the transmission plane of the polarizer-analyzer 9 (fig. 2) at an angle $\theta = 0^\circ$ and after that measure the distribution of intensity $I_0(x, y)$ of the laser field (fig. 3).

— Second one — rotate the polarizer by an angle $\theta = 90^\circ$ and after that measure the coordinate distribution of intensity $I_{90}(x, y)$ (fig. 4).

Based on the definition (1) of the Stokes vector S , we can find second parameter S_2 (fig. 5)

$$S_2 = I_0 - I_{90}. \quad (1)$$

— Next: orient the polarizer plane at an angle $\theta = 45^\circ$ and measure the coordinate distribution $I_{45}(x, y)$ (fig. 6).

— After that: rotate the polarizer by an angle $\theta = 135^\circ$ and measure the coordinate intensity distribution $I_{135}(x, y)$ (fig. 7).

Definition for the finding the third S_3 Stokes parameter (fig. 8):

$$S_3 = I_{45} - I_{135}. \quad (2)$$

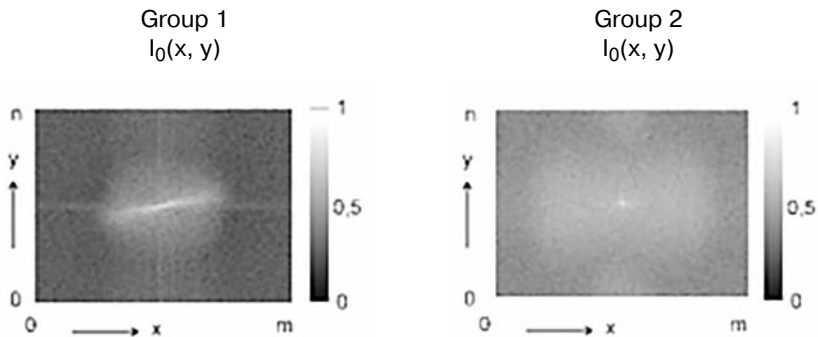


Fig. 3. Coordinate distribution of intensity of the polarization filtered field in the Fourier plane $I_0(x, y)$



— Measurement of the 4th parameter of the Stokes vector is carried out by placing a quarter-wave plate 8 on the path of the laser so-

urce (fig. 2) so that its maximum velocity axis is oriented at an angle 0° . We can orient the transmission plane of the analyzer 9 at an angle

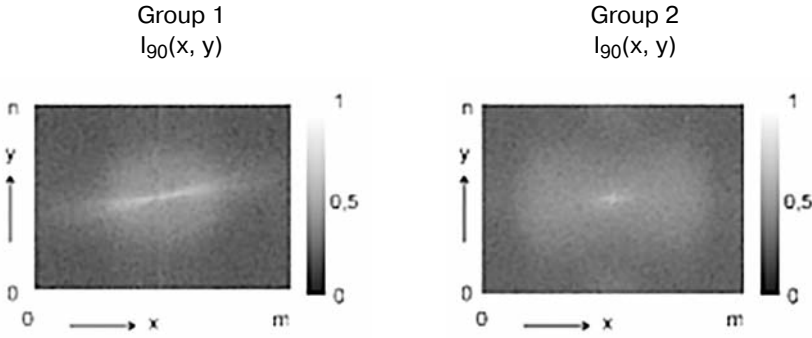


Fig. 4. Coordinate distributions of intensity of the polarization filtered field in the Fourier plane $I_{90}(x, y)$

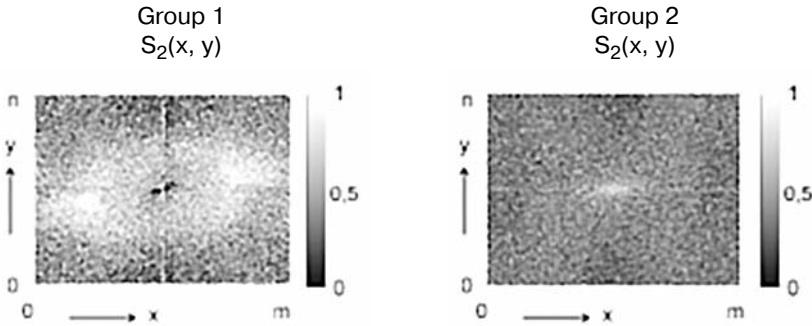


Fig. 5. Two-dimensional distributions of the 2nd parameter of the Stokes vector $S_2(x, y)$ of the field in the Fourier plane

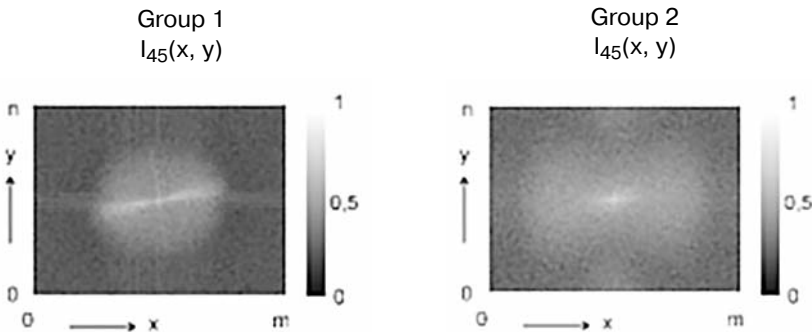


Fig. 6. Coordinate intensity distributions of the polarization filtered field in the Fourier plane $I_{45}(x, y)$



$\theta = 45^\circ$ and after that we can measure the intensity coordinate distribution of the right-circularly polarized radiation $I_{\text{right}}(x, y)$ (fig. 9).

— After that: orient the plane of the polarizer relative to the orientation of the axis of the quarter-wave plate at an angle $\theta = 135^\circ$ and mea-

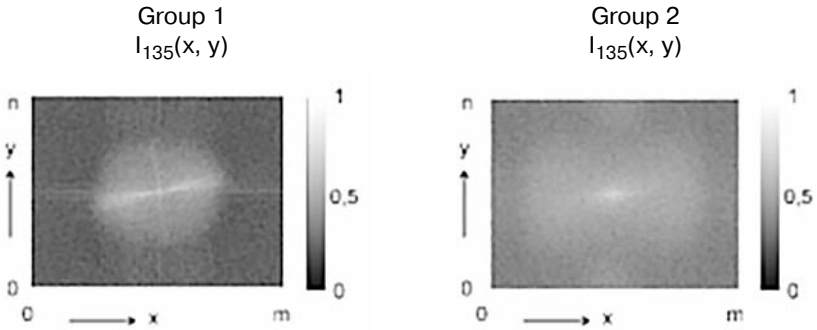


Fig. 7. Coordinate intensity distributions of the polarization filtered field in the Fourier plane $I_{135}(x, y)$

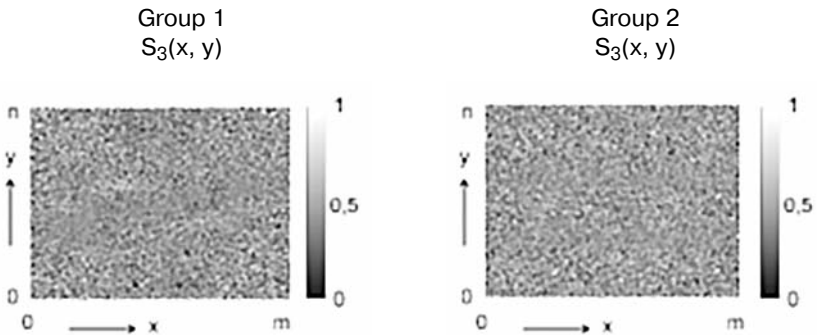


Fig. 8. Two-dimensional distributions of the 3rd Stokes vector parameter of the laser field in the Fourier plane

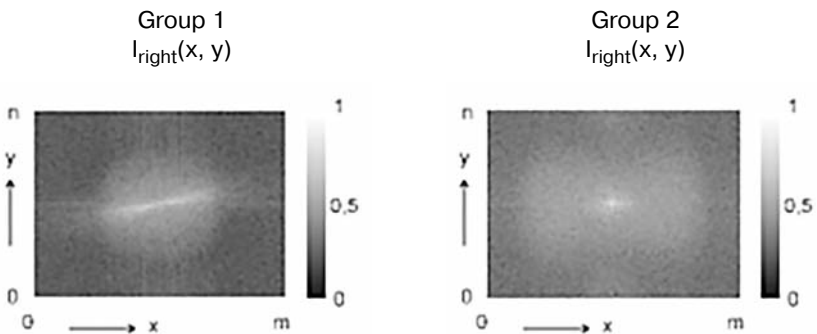


Fig. 9. Coordinate intensity distributions of the polarization filtered field in the Fourier plane $I_{\text{right}}(x, y)$



sure the corresponding intensity distributions of left-hand circularly polarized radiation $I_{\text{left}}(x, y)$ in laser images (fig. 10).

— Determine the coordinate distribution of the 4th parameter of the Stokes vector of laser images (fig. 11).

$$S_4 = I_{\text{right}} - I_{\text{left}}. \quad (3)$$

Based on deviations

$$\alpha = 0,5 \arctg \frac{S_3}{S_2}; \quad (4)$$

$$\beta = 0,5 \arcsin \frac{S_4}{S_1}. \quad (5)$$

we calculate the coordinate distributions of the azimuths $\alpha(x, y)$ and polarization ellipticity $\beta(x, y)$ of polyethylene samples laser images of from both groups.

Results

On figure 12, 13 shows a series of Fourier transform polarization maps (FIPM) of the azimuth (fig. 12) and ellipticity (fig. 13) of the polarization of laser radiation, which is transformed by a transformed optically inhomogeneous ordered grid.

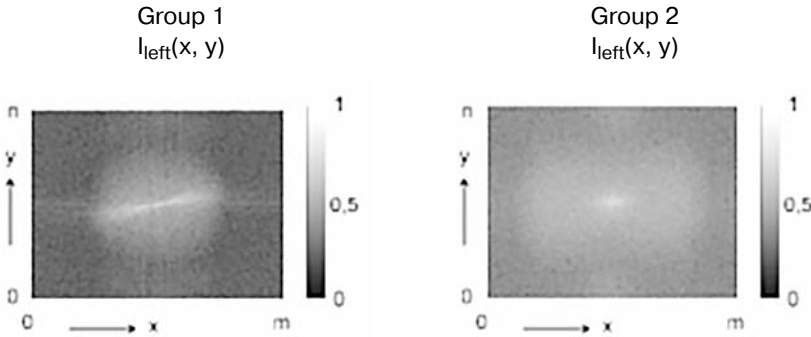


Fig. 10. Coordinate intensity distributions of the polarization filtered field in the Fourier plane $I_{\text{left}}(x, y)$

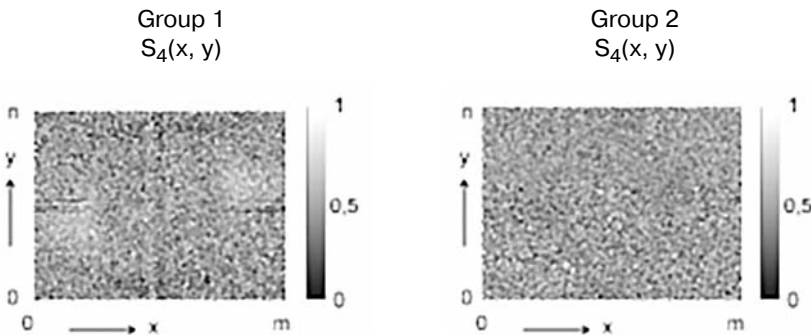


Fig. 11. Two-dimensional distributions of the 4th parameter of the laser field Stokes vector in the Fourier plane



Discussion

To obtain objective criteria for evaluating the polarization maps of Fourier images by using statistical analysis, we determined a set of values of the mean, variance, asymmetry, and kurtosis, which characterize the following spatial-frequency distributions of polarization images of polyethylene film samples.

The results of this analysis are presented and systematized in table.

Thus, the conducted experimental studies have shown the presence of a polarization-inhomogeneous structure of real polycrystalline networks of polymeric materials, and also confirmed the validity of the proposed modeling of their optical-anisotropic properties.

Different types of birefringent architectonics of different types of polymeric materials are characterized by different values of statistical moments of 1–4 orders. The difference between the moments was up to 4 times.

Conclusions

1. A relationship has been found between a set of statistical moments of the 1st–4th orders, which characterize the coordinate distributions of the azimuth and ellipticity of the polarization of the Fourier spectra of inhomogeneous images of polyethylene samples, as well as the parameters of the optical anisotropy of polycrystalline polymer networks.

2. The rationale for this relationship is based on the following factors:

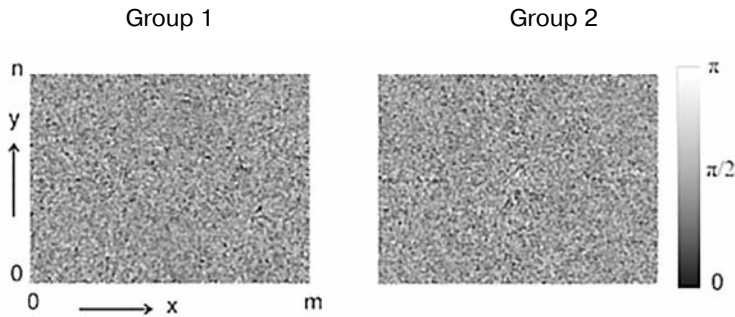


Fig. 12. FIPM of the azimuths $\alpha(x, y)$ of polarization

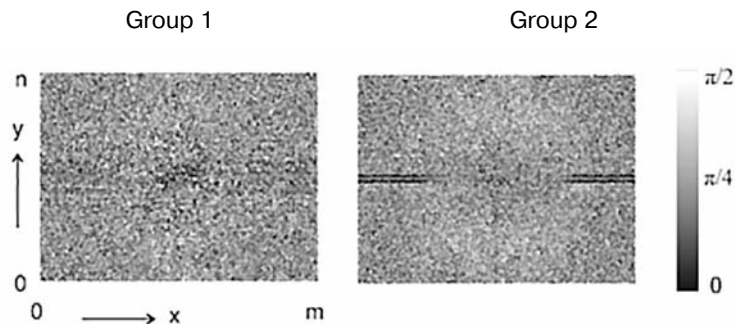


Fig. 13. FIPM of the ellipticities $\beta(x, y)$ of polarization



Statistical moments of the 1st–4th order of the distributions of the azimuth $\alpha(x, y)$ and ellipticity $\beta(x, y)$ of polarization

M_i	$\alpha(x, y)$ (number of samples — 18)	$\beta(x, y)$ (number of samples — 18)
M_1	0,18±0,015	0,09±0,006
M_2	0,13±0,010	0,11±0,008
M_3	0,67±0,05	0,23±0,018
M_4	1,14±0,11	0,42±0,031

a) the reason for the formation of the polarization structure of the Fourier spectrum of the laser image of the polymer grid is the superposition of differently polarized partial coherent waves, which are formed by different-scale partial optically inhomogeneous grids;

b) the main mechanisms for the formation of the coordinate distributions of the polarization azimuth maps of the Fourier image of the laser image are the ratios between

0–90 amplitude components, due to the features of the spatial-frequency spectra of the crystal structure with different types of birefringence;

c) the main mechanisms for the formation of distributions of the polarization ellipticity maps of the Fourier image of the laser image are phase modulations due to both the birefringence of the crystal structure and the optical characteristics of interfering partial waves.

References

1. Tuchin, V. V. (2004). *Handbook of coherent-domain optical methods. Biomedical diagnostics, environmental and material science*. Boston: Kluwer Academic Publishers, 868 p.
2. Sankaran, V., Everett, M. J., Maitland, D. J., & Walsh, J. T. (1999). Comparison of polarized-light propagation in biological tissue and phantoms. *Opt. Lett.*, Vol. 24, 1044–1046.
3. (2002). *Handbook of Optical Coherence Tomography* / edited by B. E. Bouma and G. J. Tear / Polarization-sensitive optical coherence tomography / de Boer, J. F., Milner, T. E., Ducros, M. G., Srinivas, S. M., & Nelson, J. S. New York: Marcel Dekker Inc., 237–274.
4. Angelsky, O. V., Tomka, Yu. Ya., Ushenko, A. G., Ushenko, Ye. G., & Ushenko, Yu. A. (2005). Investigation of 2D Mueller matrix structure of biological tissues for preclinical diagnostics of their pathological states. *J. Phys. D: Appl. Phys.*, Vol. 38, 4227–4235.
5. Mendoza-Galván, A., Tejeda-Galán, T., Domínguez-Gómez, A. B., Mauricio-Sánchez, R. A., Järrendahl, K.; Arwin, H. (2019). *Linear Birefringent Films of Cellulose Nanocrystals Produced by Dip-Coating*. *Nanomaterials*, 9, 45.
6. Kim, D. H. & Song, Y. S. (2015). Anisotropic optical film embedded with cellulose nanowhisker. *Carbohydrate Polymers*, Vol. 130, 448–454.



7. Furchner, A., & Hinrichs, K. (2022). Crosspolarization with imperfect infrared polarizers. *Thin Solid Films*, Vol. 763, 139560.
8. Miller, S. Jiang, L., & Pau, S. (2022). Birefringent coating to remove polarization aberrations. *Opt. Express*, 30, 20629–20646.
9. Hinrichs, K., Blevins, B., Furchner, A., Yadavalli, N. S., & Minko, S. (2022). Infrared polarimetry: Anisotropy of polymer nanofibers. *Micro and Nano Engineering*, Vol. 14, 100116.
10. Jiang, L. et al (June 15, 2022). SmartPrint Single-Mode Flexible Polymer Optical Interconnect for High Density Integrated Photonics. *Journal of Lightwave Technology*, Vol. 40, no. 12, 3839–3844, 15.

Запропоновано новий метод Стокс поляриметрії, який є більш інформативним у плані представлення оптично неоднорідних структур шляхом просторово-когерентної фільтрації.

Ключові слова: прикладне програмування; опрацювання графічної інформації; метрологія та стандартизація; поліграфічні пакувальні матеріали, матеріалознавство.

Надійшла до редакції 14.11.22